Check for updates

Wrong-way migrations of benthic species driven by ocean warming and larval transport

Heidi L. Fuchs [1] ✉, Robert J. Chant[1], Elias J. Hunter [1], Enrique N. Curchitser [2], Gregory P. Gerbi[3] and Emily Y. Chen [1]

Ocean warming has predictably driven some marine species to migrate polewards or to deeper water, matching rates of environmental temperature change (climate velocity) to remain at tolerable temperatures. Most species conforming to expectations are fish and other strong swimmers that can respond to temperature change by migrating as adults. On the Northwest Atlantic continental shelf, however, many benthic invertebrates' ranges have instead shifted southwards and into shallower, warmer water. We tested whether these 'wrong-way' migrations could arise from warming-induced changes in the timing of spawning (phenology) and transport of drifting larvae. The results showed that larvae spawned earlier in the year encounter more downwelling-favourable winds and river discharge that drive transport onshore and southwards. Phenology and transport explained most observed range shifts, whereas climate velocity was a poor predictor. This study reveals a physical mechanism that counterintuitively pushes benthic species, including commercial shellfish, into warmer regions with higher mortality.

Ocean warming has predictably driven some marine species to migrate polewards or to deeper water[1–3], matching rates of environmental temperature change (climate velocity) to remain at tolerable temperatures[4]. The paradigm that species' ranges are controlled by thermal tolerance[5] is intuitive but fails to explain ranges shifting unexpectedly towards warmer temperatures. Counterintuitive shifts have been explained in terms of species-level characteristics and local variation in climate velocities[4], but no compelling mechanisms have emerged. 'Wrong-way' migrations are common among bottom-dwelling invertebrates that lack adult mobility and instead disperse as microscopic larvae. Larvae swim weakly and are at the mercy of complex water motions[6,7] and currents that can transport them hundreds or even thousands of kilometres. Despite being highly dispersive, benthic species may be unable to follow climate velocities when the physics-driven transport of larvae opposes temperature-driven shifts of adult ranges[8,9]. Changes in planktonic transport have far-reaching consequences for community structure[10] and biogeography but are among the least understood impacts of warming on marine systems[11]. Here we identify mechanisms linking larval transport to wrong-way migrations along the US Northwest Atlantic (NWA) continental shelf (Fig. 1a), where rapid warming has induced range shifts that forecast the global redistribution of benthic species.

Larval transport could be impacted by ocean warming via changes in spawning phenology. Most temperate species begin spawning in spring and summer[12], but reproductive timing is often driven by temperature[13,14], and recent warming has induced some species to spawn earlier[15,16]. Phenology probably has changed over time in the Middle Atlantic Bight (MAB), an area of the NWA continental shelf that has warmed three times faster than the global average rate[17,18]. The spawning of benthic species is most affected by temperature in bottom water, which lags behind surface temperature seasonally[19,20] but has warmed by ~2 °C since the 1960s (Fig. 1). This warming could induce MAB species to spawn earlier in the year, exposing larvae to different winds and river discharge that drive physical transport on the shelf (Fig. 2).

Spawning times affect how larvae are transported by seasonally variable, wind-driven upwelling and downwelling. Along the US East Coast, upwelling is driven by northward winds that draw bottom water onshore and force surface waters offshore, while downwelling reverses the pattern. Strong upwelling can send larvae offshore and limit recruitment[21,22], whereas downwelling can concentrate larvae nearshore[23]. However, the transport direction depends on whether larvae are nearer the surface or bottom[24,25], and debate continues over how upwelling affects cross-shelf delivery of larvae to the coast[26,27]. Less attention has been given to how upwelling transports larvae along-shelf. In the MAB, summer winds are along-shelf and upwelling-favourable, driving currents predominantly across-shelf, but spring and autumn winds are oblique to the coast and downwelling-favourable, driving currents predominantly along-shelf to the southwest (down-shelf, Fig. 2)[28,29]. Larvae spawned earlier in spring would experience stronger downwelling and onshore transport near the surface, coupled with faster transport down the shelf.

MAB transport also reflects seasonal variability in river discharge that generates cross-shelf buoyancy gradients and drives depth-averaged, along-shelf currents shorewards of the 60 m isobath[28]. In spring, high river discharge produces strong down-shelf flow, whereas in late summer, low discharge reduces the cross-shore buoyancy gradient and enables down-shelf flows to weaken[28] or sometimes be reversed by winds[30] (Fig. 2). The spring peak in discharge coincides with downwelling winds and the prevailing down-shelf flow that transports material southwards to warmer latitudes (Fig. 2). A phenological shift in spawning from summer to spring would thus intensify larval transport both onshore and down-shelf, causing a drift in recruitment patterns that could be reflected in adult distributions.

We tested this hypothesis by analysing range shifts of benthic invertebrates using occurrence data in the NWA and MAB from 1950 to 2015 (Supplementary Table 1). In both the NWA and MAB, most species shifted southwards, westwards and into shallower water (Fig. 3 and Extended Data Fig. 1). At species' occurrence

¹Department of Marine and Coastal Sciences, Rutgers University, New Brunswick, NJ, USA. ²Department of Environmental Sciences, Rutgers University, New Brunswick, NJ, USA. ³Physics Department, Skidmore College, Saratoga Springs, NY, USA. ✉e-mail: hfuchs@marine.rutgers.edu
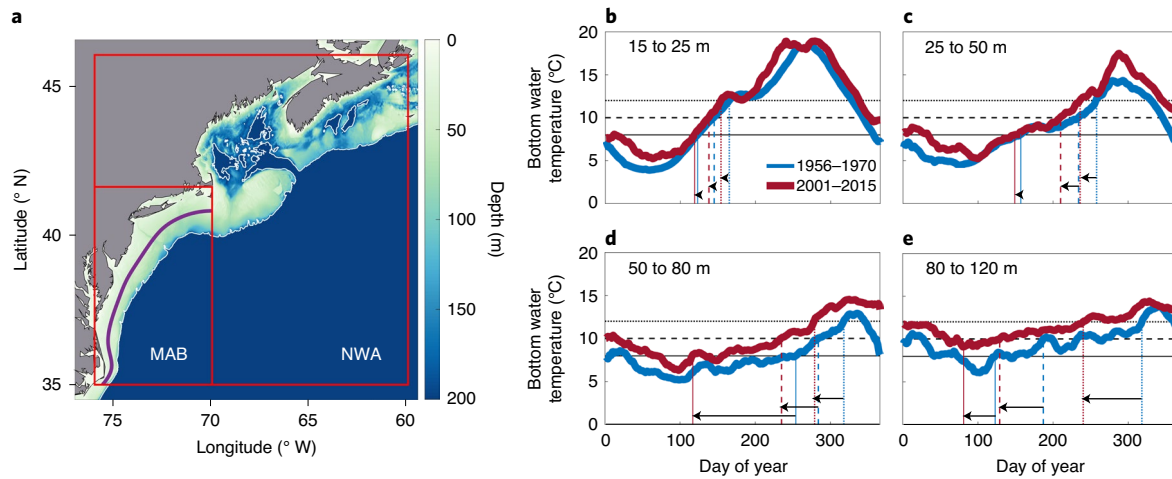
Fig. 1 | Spawning phenology would shift due to warming in the NWA and MAB regions. a, Map showing the NWA (outer rectangle) and MAB (inner rectangle). The purple line is the shelf axis defining cross-shelf and along-shelf positions, the background colour indicates depth (m) and the white contour is the 200 m isobath. **b–e**, In the MAB over four depth ranges (15 to 25 m (**b**), 25 to 50 m (**c**), 50 to 80 m (**d**) and 80 to 120 m (**e**)), the mean bottom water temperatures were ~2 °C higher in 2001–2015 (red) than in 1956–1970 (blue), while the onset of potential spawning temperatures (8 °C, thin solid lines; 10 °C, dashed lines; 12 °C, dotted lines) shifted earlier in the year (black arrows).
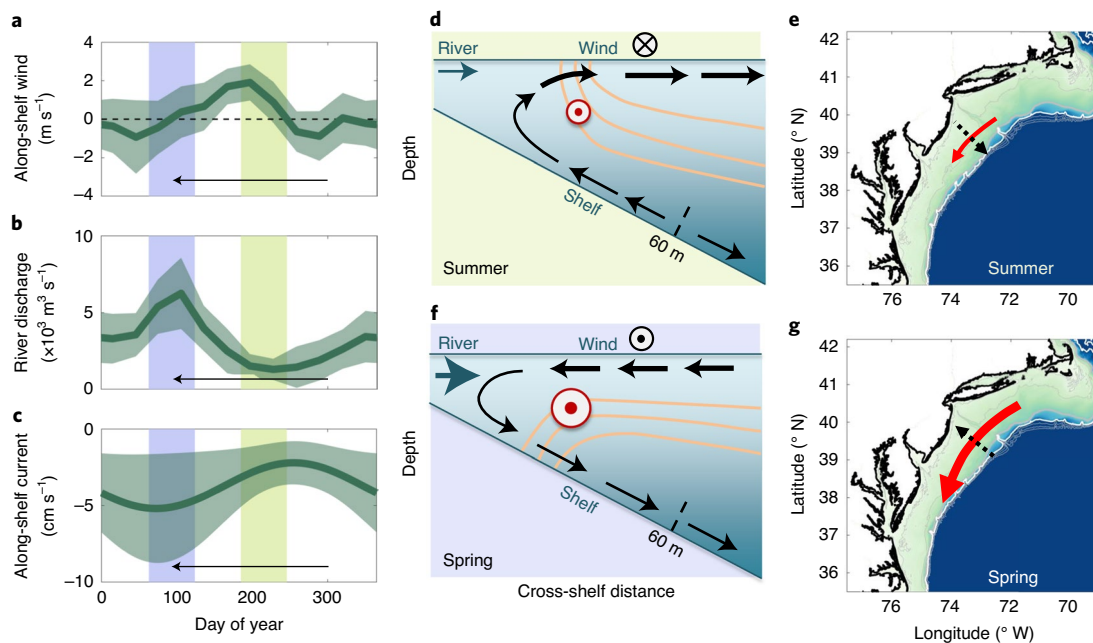

Fig. 2 | Phenological shifts from summer to spring would expose larvae to more onshore, down-shelf transport. a–c, Along-shelf winds (**a**) are downwelling-favourable (negative) in spring and autumn and upwelling-favourable in summer, while river discharge (**b**) is highest in spring and lowest in summer. The resulting depth-averaged, along-shelf currents (**c**) are the most negative (down-shelf) in spring. The mean ±1 s.d. is shown. The shading highlights mid-spring (March to April, purple) and mid-summer (July to August, green). **d–g**, Cartoons show MAB summer (**d,e**) and spring (**f,g**) circulation. Directions are indicated by the arrows and circles (⊙, out of page; ⊗, into page); the arrow thicknesses indicate the relative magnitudes. Along-shelf transport (red symbols and arrows) is the mean depth average. Cross-shelf transport (black arrows) varies with depth; surface transport (dashed arrows) is shown in **e,g**.

locations, we estimated the annual average bottom-water temperatures using a long-term, data-corrected model temperature record (Extended Data Fig. 2). The results showed that two-thirds of species' ranges have gotten warmer (Fig. 3 and Extended Data Fig. 1), and some ranges warmed despite shifting northwards because the distributions became shallower (see, for example, Extended Data Fig. 3 and Supplementary Fig. 1). Of the warming ranges, nearly

all have warmed faster—some up to ten times faster—than the temperature records themselves, indicating that ranges warmed mainly from range shifting rather than from climate change.

These range shifts were counterintuitive, so we tested whether they were better predicted by climate velocity or by spawning phenology. Climate velocities were generally smaller than and uncorrelated with range shift velocities (Fig. 3 and Extended Data Figs. 4
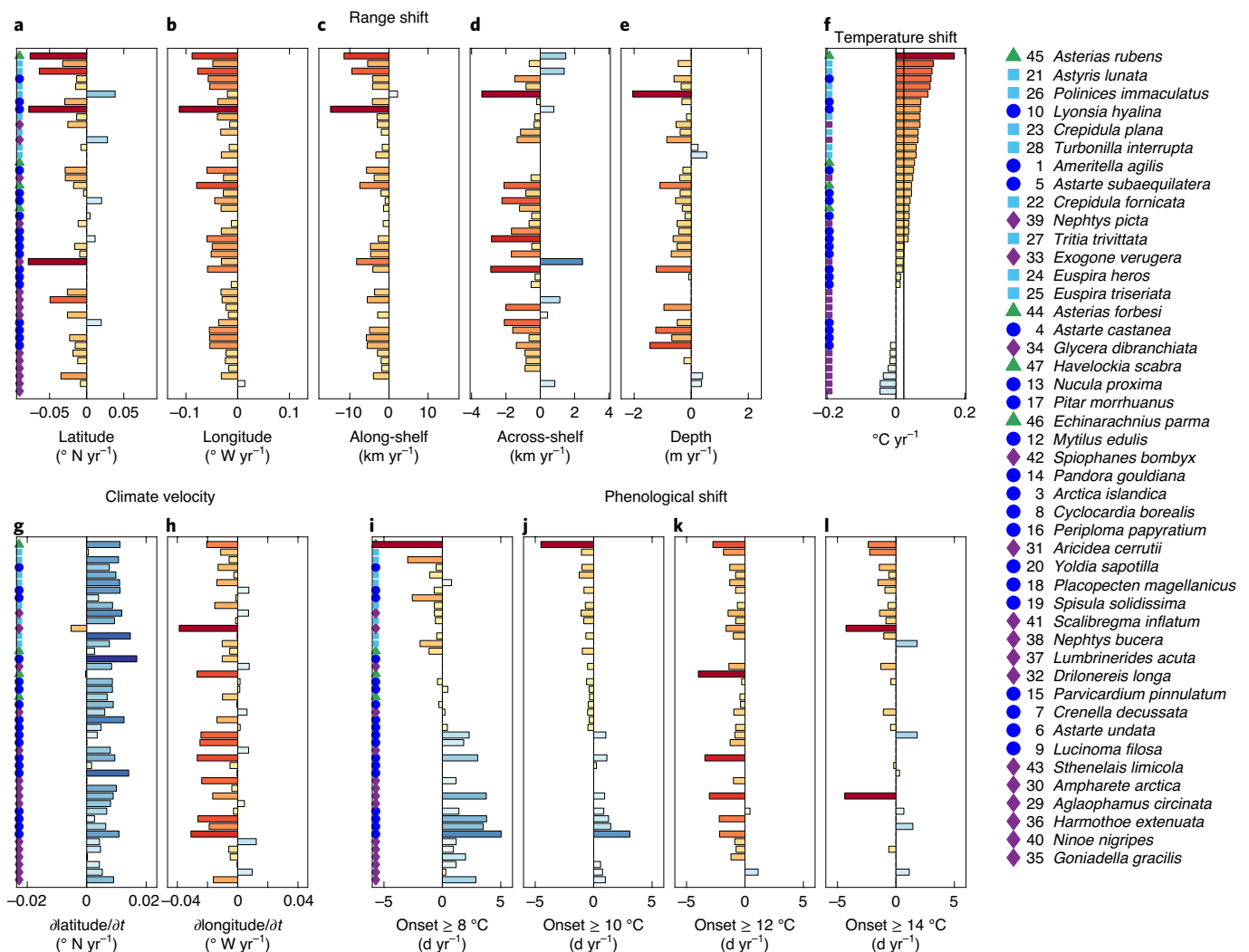
Fig. 3 | In the MAB, most ranges shifted southwest, down-shelf and onshore to shallower, warmer regions with earlier spawning onset. a–e, Trends in latitude (**a**), longitude (**b**), along-shelf (**c**) and across-shelf (**d**) distances, and depths (**e**) computed from occurrence locations versus year for each species. **f–l**, Bottom water temperature trends (**f**), mean climate velocities (**g,h**) and trends in onset dates for spawning at temperatures 8 to 14 °C (**i–l**) computed from model hindcast at occurrence locations versus year. The vertical line in **f** indicates the mean warming trend across the NWA. Trends significant at $\alpha = 0.05$ are included. The symbols indicate taxa (blue circles for bivalves, cyan squares for gastropods, purple diamonds for polychaetes and green triangles for echinoderms). The legend indicates species, omitting species that are sparse in the MAB (the details are in Supplementary Table 1).

and 5). In the MAB, latitudinal climate velocities were mostly northward, whereas range shifts were mostly southward. Range shift velocities in the MAB were weakly correlated with climate velocities in longitude (∂longitude/∂t), but climate velocities diverged at mid-shelf, and this correlation would have resulted coincidentally as ranges shifted from the outer shelf (where values of ∂longitude/∂t are positive) to the inner shelf (where values of ∂longitude/∂t are negative) (Extended Data Fig. 4). Most species spawn at unknown temperatures, so we analysed phenological shifts using four possible thresholds: 8 °C, 10 °C, 12 °C and 14 °C (Supplementary Table 2). This analysis excluded the Gulf of Maine, where temperatures are generally <10 °C, focusing on the MAB where phenological shifts are pronounced (Extended Data Fig. 6). As species shifted into warmer water, the onset dates for spawning temperature thresholds likewise shifted earlier in the year (Fig. 3). In the MAB, earlier spawning was correlated with range shifts to the southwest and down the shelf (Extended Data Fig. 7). Overall, the observed range shifts—particularly with respect to latitude and along the shelf—were best predicted by spawning phenology.

Changing phenology may cause adult ranges to shift by altering larval supply or advection. Distributions in the MAB could remain stable if there were a steady supply of larvae, perhaps including those from upstream populations in the Gulf of Maine or Georges Bank. Many upstream species' distributions have also shifted into shallower water (Extended Data Fig. 3), potentially removing a source of larvae from the northern and outer parts of the MAB shelf. In the MAB, the prevailing along-shelf flow is always to the southwest, yet species' ranges could remain stable if down-shelf larval advection were partially offset by horizontal dispersion[31,32]. Dispersion is also affected by winds and river discharge, but neither forcing mechanism has changed over the long term in the region (see 'Transport mechanisms in the MAB'), and we assume that larval dispersal has remained steady. Instead, range shifts probably resulted from phenologically driven changes in along-shelf larval advection.

To test this possibility, we quantified the long-term change in mean transport velocity. From 1960 to 2010 in the MAB, warming bottom waters would have induced earlier spawning, aligning larval release more closely with peak downwelling winds and river
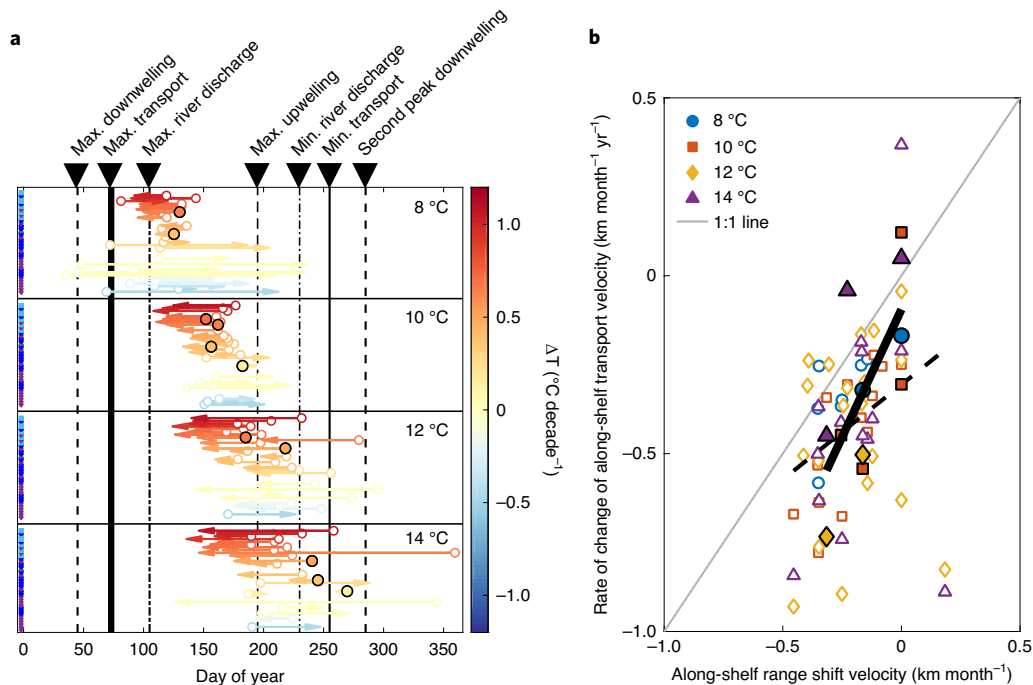
Fig. 4 | Most phenological shifts would result in faster larval transport down the shelf, explaining adults' along-shelf range shifts. a, Estimated shifts in spawning onset (arrows) from 1960 to 2010 at four temperature thresholds in the MAB. The species are ordered as in Fig. 3. Trends significant at $\alpha = 0.05$ are included. Species sparse in the MAB or after 1990 (Supplementary Table 1) are omitted. The colours indicate temperature trends. The vertical lines mark seasonal extremes of mean along-shelf winds, river discharge and down-shelf transport (Fig. 1). **b**, Estimated rates of change of larval transport velocities versus observed along-shelf range shift velocities for species with phenological shifts to earlier in the year (open symbols; dashed line; $P = 0.01$; $R^2 = 0.11$). The solid symbols in both panels differentiate estimates for species' known spawning temperatures (solid line; $P = 0.02$; $R^2 = 0.47$).

discharge and exposing larvae to progressively more negative (southward) along-shelf flows (Fig. 4a). We used estimated spawning dates and observed along-shelf currents to quantify the mean larval transport velocities within the first month after spawning. Down-shelf transport generally increased over these five decades (Extended Data Fig. 8). These changes in along-shelf transport were correlated with range shift velocities using all estimates where spawning shifted earlier in the year and using estimates at seven species' known spawning temperatures (Fig. 4b). The correlations were insensitive to assumed dispersal times of two weeks to two months. We therefore attribute the observed range shifts to warming-induced, earlier spawning that exposed larvae to more downwelling and down-shelf flow, enhancing dispersal to shallower depths and southern latitudes, where adult ranges became warmer. Warmer regions also reach temperature thresholds earlier in the year (Extended Data Fig. 6), magnifying the phenological change and creating a feedback between warming and southwesterly migration.

These findings oppose trends observed in fish, challenging the generality that marine species are better than terrestrial species at following climate velocity[4]. Many adult fish are mobile enough to control their ranges behaviourally. In contrast, most benthic species are sedentary or fixed to the seabed as adults, dispersing only as tiny larvae adrift on ocean currents. Larvae can exploit directional currents by swimming vertically, but many larval behaviours would have evolved during summer upwelling and may be poorly adapted for spring downwelling. Physical transport is so variable and complex[6,7] that larval behaviours almost certainly evolve slower than the current pace of warming.

Larval behaviours may ultimately explain why the observed rates of wrong-way migration exceed the inferred increases in down-shelf larval transport velocity (Fig. 4b). We estimated transport rates using harmonic fits to along-shelf currents averaged over the water

depth (Methods), but compared with the depth average, currents at the surface are more seasonally variable and about twice as fast[29]. The increases in down-shelf transport are therefore probably underestimated for any larvae whose behaviours concentrate them in the upper water column. Moreover, episodic winds and flooding events can drive even faster surface flows and may further influence larval transport through behavioural responses to physical processes such as turbulence and waves[33], which also vary seasonally. We are assessing how behaviour modifies larval transport using realistic numerical simulations in a separate study.

The physical control of dispersal could lead to paradoxical range compression and 'death by downwelling'. Marine species generally fill their tolerable range of latitudes, and tolerable latitude bands can grow wider as warming shifts them polewards[3,34]. However, phenological changes in larval transport could prevent benthic species from reaching more northern latitudes or cooler depths, concentrating animals at warmer ends of their thermal niches (see, for example, Extended Data Fig. 9) and shrinking occupied ranges. We estimated that species' thermally tolerable areas slightly increased from 1951–1980 to 1981–2010, whereas in the MAB their occupied areas shrank by an average of 10% as ranges shifted onshore (Extended Data Fig. 10). This range compression is similar to the escalator-to-extinction effect, where increasing temperatures at high altitudes drive birds and butterflies upslope until species are extirpated[35,36]. Yet the downwelling effect is more insidious, because benthic species' ranges shrank even as habitable areas grew, and ranges shrank towards rather than away from warmer areas where mortality is the highest.

As climate change reduces yields from traditional fisheries[37], the seafood industry may rely more heavily on invertebrates, including shellfish, that disperse as larvae. Of the commercial species included here, scallops (*Placopecten magellanicus*) spawn at a wide range of

temperatures, and their ranges have remained relatively constant. In contrast, clams (*Arctica islandica* and *Spisula solidissima*) and mussels (*Mytilus edulis*) spawn primarily at low temperatures, and their ranges have warmed and contracted. Phenological changes in spawning could profoundly impact larval transport in temperate upwelling zones that support major fisheries. Compared with the MAB, major upwelling zones such as the California Current have stronger and more seasonally variable currents with reverse directionality relative to the coastline. Also, unlike the MAB, major upwelling zones are among regions where wind speeds have increased since the 1980s[38]. These differences make it impossible to generalize how phenological changes will alter larval transport more globally, and regional processes must be investigated to accurately forecast the impacts of warming on benthic species.

Online content

Any methods, additional references, Nature Research reporting summaries, source data, extended data, supplementary information, acknowledgements, peer review information; details of author contributions and competing interests; and statements of data and code availability are available at https://doi.org/10.1038/s41558-020-0894-x.

References

1. Perry, A. L., Low, P. J., Ellis, J. R. & Reynolds, J. D. Climate change and distribution shifts in marine fishes. *Science* **308**, 1912–1915 (2005).
2. Dulvy, N. K. et al. Climate change and deepening of the North Sea fish assemblage: a biotic indicator of warming seas. *J. Appl. Ecol.* **45**, 1029–1039 (2008).
3. Sunday, J. M., Bates, A. E. & Dulvy, N. K. Thermal tolerance and the global redistribution of animals. *Nat. Clim. Change* **2**, 686–690 (2012).
4. Pinsky, M. L., Worm, B., Fogarty, M. J., Sarmiento, J. L. & Levin, S. A. Marine taxa track local climate velocities. *Science* **341**, 1239–1242 (2013).
5. Hutchins, L. W. The bases for temperature zonation in geographical distribution. *Ecol. Monogr.* **17**, 325–335 (1947).
6. Pineda, J., Reyns, N. B. & Starczak, V. R. Complexity and simplification in understanding recruitment in benthic populations. *Pop. Ecol.* **51**, 17–32 (2009).
7. Morgan, S. G., Shanks, A. L., MacMahan, J. H., Reniers, A. J. H. M. & Feddersen, F. Planktonic subsidies to surf-zone and intertidal communities. *Annu. Rev. Mar. Sci.* **10**, 345–369 (2018).
8. Gaylord, B. & Gaines, S. D. Temperature or transport? Range limits in marine species mediated solely by flow. *Am. Nat.* **155**, 769–789 (2000).
9. García Molinos, J., Burrows, M. T. & Poloczanska, E. S. Ocean currents modify the coupling between climate change and biogeographical shifts. *Sci. Rep.* **7**, 1332 (2017).
10. Kumagai, N. H. et al. Ocean currents and herbivory drive macroalgae-to-coral community shift under climate warming. *Proc. Natl Acad. Sci. USA* **115**, 8990–8995 (2017).
11. Harley, C. D. G. et al. The impacts of climate change in coastal marine systems. *Ecol. Lett.* **9**, 228–241 (2006).
12. Strathmann, M. F. *Reproduction and Development of Marine Invertebrates of the Northern Pacific Coast* (Univ. of Washington Press, 1987).
13. Thorson, G. Reproductive and larval ecology of marine bottom invertebrates. *Biol. Rev.* **25**, 1–45 (1950).
14. Olive, P. J. W. Annual breeding cycles in marine invertebrates and environmental temperature: probing the proximate and ultimate causes of reproductive synchrony. *J. Therm. Biol.* **20**, 79–90 (1995).
15. Philippart, C. J. M. et al. Climate-related changes in recruitment of the bivalve *Macoma balthica. Limnol. Oceanogr.* **48**, 2171–2185 (2003).
16. Asch, R. G. Climate change and decadal shifts in the phenology of larval fishes in the California Current Ecosystem. *Proc. Natl Acad. Sci. USA* **112**, E4065–E4074 (2015).
17. Shearman, R. K. & Lentz, S. J. Long-term sea surface temperature variability along the U.S. East Coast. *J. Phys. Oceanogr.* **40**, 1004–1017 (2010).
18. Saba, V. S. et al. Enhanced warming of the northwest Atlantic Ocean under climate change. *J. Geophys. Res. Oceans* **121**, 118–132 (2016).
19. Castelao, R., Glenn, S. & Schofield, O. Temperature, salinity, and density variability in the central Middle Atlantic Bight. *J. Geophys. Res.* **115**, C10005 (2010).
20. Richaud, B., Kwon, Y.-O., Joyce, T. M., Fratantoni, P. S. & Lentz, S. J. Surface and bottom temperature and salinity climatology along the continental shelf off the Canadian and U.S. East Coasts. *Cont. Shelf Res.* **124**, 165–181 (2016).
21. Roughgarden, J., Gaines, S. & Possingham, H. Recruitment dynamics in complex life cycles. *Science* **241**, 1460–1466 (1988).
22. Connolly, S. R., Menge, B. A. & Roughgarden, J. A latitudinal gradient in recruitment of intertidal invertebrates in the northeast Pacific Ocean. *Ecology* **82**, 1799–1813 (2001).
23. Ma, H., Grassle, J. P. & Chant, R. J. Vertical distribution of bivalve larvae along a cross-shelf transect during summer upwelling and downwelling. *Mar. Biol.* **149**, 1123–1138 (2006).
24. Shanks, A. L. & Brink, L. Upwelling, downwelling, and cross-shelf transport of bivalve larvae: test of a hypothesis. *Mar. Ecol. Prog. Ser.* **302**, 1–12 (2005).
25. Drake, P. T., Edwards, C. A., Morgan, S. G. & Dever, E. P. Influence of larval behavior on transport and population connectivity in a realistic simulation of the California Current System. *J. Mar. Res.* **71**, 317–350 (2013).
26. Shanks, A. L. & Morgan, S. G. Testing the intermittent upwelling hypothesis: upwelling, downwelling, and subsidies to the intertidal zone. *Ecol. Monogr.* **88**, 22–35 (2018).
27. Menge, B. A. & Menge, D. N. L. Testing the intermittent upwelling hypothesis: comment. *Ecology* **100**, e02476 (2019).
28. Lentz, S. J. Seasonal variations in the circulation over the Middle Atlantic Bight continental shelf. *J. Phys. Oceanogr.* **38**, 1486–1500 (2008).
29. Gong, D., Kohut, J. T. & Glenn, S. M. Seasonal climatology of wind-driven circulation on the New Jersey Shelf. *J. Geophys. Res.* **115**, C04006 (2010).
30. Whitney, M. M. & Garvine, R. W. Wind influence on a coastal buoyant outflow. *J. Geophys. Res.* **110**, C03014 (2005).
31. Largier, J. L. Considerations in estimating larval dispersal distances from oceanographic data. *Ecol. Appl.* **13**, S71–S89 (2003).
32. Byers, J. E. & Pringle, J. M. Going against the flow: retention, range limits and invasions in advective environments. *Mar. Ecol. Prog. Ser.* **313**, 27–41 (2006).
33. Fuchs, H. L., Gerbi, G. P., Hunter, E. J. & Christman, A. J. Waves cue distinct behaviors and differentiate transport of congeneric snail larvae from sheltered versus wavy habitats. *Proc. Natl Acad. Sci. USA* **115**, E7532–E7540 (2018).
34. Sunday, J. M., Bates, A. E. & Dulvy, N. K. Global analysis of thermal tolerance and latitude in ectotherms. *Proc. R. Soc. B* **278**, 1823–1830 (2011).
35. Wilson, R. J. et al. Changes to the elevational limits and extent of species ranges associated with climate change. *Ecol. Lett.* **8**, 1138–1146 (2005).
36. Freeman, B. G., Scholer, M. N., Ruiz-Guttierrez, V. & Fitzpatrick, J. W. Climate change causes upslope shifts and mountaintop extirpations in a tropical bird community. *Proc. Natl Acad. Sci. USA* **115**, 11982–11987 (2018).
37. Free, C. M. et al. Impacts of historical warming on fisheries production. *Science* **363**, 979–983 (2019).
38. Young, I. R. & Ribal, A. Multiplatform evaluation of global trends in wind speed and wave height. *Science* **364**, 548–552 (2019).

Methods

Study design. This study related species' range shifts to associated changes in bottom-water temperature, spawning phenology and physical transport mechanisms. We used data from depths <200 m on the continental shelf over two geographic areas. The NWA region extended from Cape Hatteras, United States, to Nova Scotia, Canada (between 35 and 46° N and 60 and 76° W), and the MAB region included only Cape Hatteras to Nantucket, United States (between 35 and 41.6° N and 76 and 70° W) (Fig. 1a). We related phenology to transport mechanisms only in the MAB region, which is warming rapidly[18] and has geometry that facilitates generalizations about physical transport along and across the shelf.

Species data. *Occurrence.* Species occurrence data were compiled from the Ocean Biogeographic Information System (OBIS)[39] using all databases contributing to each species. Occurrence data provide positive information only and may underestimate species' actual ranges. Although these presence-only data have limitations—for example, they can be used to infer extinction but not colonization[40]—they are the best available resource for estimating ranges of unfished marine invertebrates. The included databases (Supplementary Table 3) varied in their sampling methods and coverage and lacked the biomass data needed to calculate range envelopes as in ref. [4], but our focus on occurrence eliminates the need to standardize abundances or biomass. To assess whether the results were biased by changes in database availability over time, we repeated our analyses (described below) using only the database with the most numerous records (NEFSC benthic database), which ended in 1989. The results were qualitatively similar using all databases versus NEFSC only, but wrong-way trends in latitude, longitude and temperature were stronger using the NEFSC subset alone (Extended Data Fig. 1 and Supplementary Fig. 2), possibly because decadal-scale temperature variability differed before and after 1990 (Extended Data Fig. 2). We used all datasets because they provide more conservative estimates of wrong-way shifts while capturing longer-term trends including the past 30 years.

Our initial species list included bivalves, gastropods, polychaetes and echinoderms listed previously as abundant in the MAB (ref. [41]). Species were excluded if their occurrence was sparse in the overall record, if their distribution was mainly estuarine or if their development was direct. Most species' distributions included only the east coast of North America, but some species were observed outside our study range (Supplementary Table 1). South of the MAB, the temperature data were too sparse to use with confidence, and north of Nova Scotia, the occurrence data were more limited by sampling surveys, so we excluded these regions from the analysis. Many species have undergone name changes, but past-name data are usually compiled in the OBIS record for the currently accepted name. *Tritia trivittata* has a separate OBIS record under the past name *Nassarius trivittatus*, so we combined the two records and report all data under *Tritia trivittata*. Our final analysis included 50 species (Supplementary Table 1).

Range shifts. The OBIS data lacked the information on abundance or biomass needed to quantify the centroids of species' distributions[4], so we assessed species' range shifts on the basis of trends in occurrence locations over time. For all species, we used occurrence data from 1950 to 2015 that included both a date and coordinates (latitude/longitude) where juveniles or adults were sampled. Where records omitted water depth, we interpolated depth from National Oceanic and Atmospheric Administration (NOAA) bathymetry[42] to the sampling coordinates. Data from deeper than 200 m were considered beyond the shelf edge and were excluded. Species with <100 records in the MAB region (Supplementary Table 1) were used only for the NWA analysis. For the NWA and MAB regions, we quantified range shifts using linear regressions of latitude, longitude and depth at occurrence locations versus year (see, for example, Supplementary Fig. 1).

In the MAB, we also quantified range shifts across and along the shelf. We defined the shelf axis as an arbitrary curve extending from 35° N to 41° N and passing approximately midway between the coastline and the shelf edge (Fig. 1a). These axis and occurrence data were first converted from latitude/longitude to Cartesian distance coordinates. The occurrence data were then converted to shelf coordinates using a normal line from each occurrence location to the along-shelf axis. For each occurrence, we defined the across-shelf coordinate x_s (negative towards the coast, consistent with longitude in the NWA) as the length of the normal line and defined the along-shelf coordinate y_s (positive up-shelf or northwards) as the point where the normal line intersected the shelf axis. For the MAB, we quantified range shifts using linear regressions of x_s and y_s versus year (see, for example, Supplementary Fig. 1).

Temperature data. We used bottom-water temperature (T_b) records to estimate three properties associated with species' occurrence locations: (1) the trends in annual average T_b experienced by benthic adults, (2) the velocities at which annual average T_b moves through space due to long-term climate change (climate velocities)[43] and (3) the trends in day of the year when T_b first hits potential thresholds to induce spawning (phenology). The first two properties require annual average temperatures, whereas the third requires daily average values of T_b that resolve seasonal climatology. We used values of T_b from model outputs after correcting them with observations.

The modelled temperatures were taken from a published, multidecadal regional ocean model (ROMS) hindcast (HC)[44–46]. The outputs included two periods (1958–2007 and 2008–2012) forced with environmental conditions from different reanalysis datasets; both sets of outputs are publicly available from the THREDDS data server at Rutgers (https://esm.rutgers.edu/). Temperatures from the bottom model level were used to represent $T_{b_{HC}}$. The model is well resolved and accurately captures the spatial and seasonal variability in T_b, but temperatures throughout the region are positively biased (too warm) and lack the observed warming trend (Extended Data Fig. 2).

The observed temperatures were taken from NOAA's publicly available World Ocean Database (WOD; https://www.nodc.noaa.gov/OC5/WOD/pr_wod.html). We used records from 1950 to 2015 and took data from the bottom 10 m to represent $T_{b_{WOD}}$. Data were omitted if the reported measurement depth was greater than the local water depth, indicating a faulty measurement, or if T_b was <0 °C or >30 °C. The WOD observations were scattered and unevenly dense in space and time (Supplementary Fig. 3), and the coarse resolution is a shortcoming of the dataset. Despite undersampling of some seasons and locations, the WOD record and model HC have long-term mean temperatures with similar spatial patterns (Extended Data Fig. 2). The two records also show similar climatology in the MAB. We averaged daily temperatures over four depth ranges (10–25 m, 25–50 m, 50–80 m and 80–120 m) for each decade, filled gaps in the WOD record using an autoregressive model, applied a median filter to remove spikes and smoothed both records using a 28-day, central moving average. The long-term changes in WOD climatology are summarized in Fig. 1b–e. The WOD and HC climatologies were similar, but the HC climatology (like the annual average temperatures) was too warm and lacked the observed warming trend. Given that seasonal cycles and spatial patterns were similar in the two records, but the WOD data were coarsely resolved, we used the WOD data only to correct the systematic regional bias and trend in the HC record.

Before we could use the WOD data for bias correction, several steps were needed to avoid overweighting heavily sampled seasons and locations. We first binned the data over 0.2-degree square grids, reflecting a compromise between bins large enough to contain many data points and small enough to resolve temperature variation associated with bathymetry. We then evened the weighting of over- and undersampled seasons within each grid cell by first computing the monthly averages and then using the monthly averages to compute the annual average temperatures. Next, we evened the spatial weighting of over- and undersampled regions for each year by interpolating the annual average temperatures to fill empty grid cells[47]. Finally, we evened the weighting of over- and undersampled years by using a moving average with a centred, 11-year window (±5 years) to compute roughly decadally averaged annual mean temperatures in each bin ($T^*_{b_{WOD}}$). These values of $T^*_{b_{WOD}}$ still contained too much spatial noise to be used with confidence for spatially resolved analyses, but they were appropriately weighted for estimating the regional warming trend.

We used the reweighted WOD data from 1958 to 2012 to correct the bias and trend in the HC. In both datasets, we calculated the spatial average annual temperature (τ) over the entire NWA region at depths ≤200 m, omitting Delaware and Chesapeake Bays:

$$\tau_{WOD}(t) = \left\langle T^*_{b_{WOD}}(x, y, t) \right\rangle \tag{1}$$

$$\tau_{HC}(t) = \left\langle T_{b_{HC}}(x, y, t) \right\rangle \tag{2}$$

where $T_{b_{HC}}$ are the annual averages from the HC, x and y are the longitude and latitude, t is the year and the angle brackets indicate spatial averaging. We then replaced the spatial average temperature trend in the HC with the one from the data:

$$T'_{b_{HC}}(x, y, t) = T_{b_{HC}}(x, y, t) - \tau_{HC}(t) + \tau_{WOD}(t) \tag{3}$$

This correction maintains the HC record's spatial variability in warming, eliminates its positive bias and corrects the mean warming trend to that of the observations: 0.021 °C yr⁻¹ (Supplementary Fig. 2). The mean warming trend is estimated over the NWA and is intermediate between the observed warming of bottom waters in the MAB (~0.04 °C yr⁻¹; Fig. 1b–e) and previously observed and modelled warming of sea surface temperature along the NWA shelf north of 36° N (ref. [17]). To quantify the temperatures experienced by adult animals, we interpolated $T'_{b_{HC}}$ to species' occurrence locations and estimated trends in species' range temperatures using linear regressions of $T'_{b_{HC}}$ at occurrence locations versus year from 1958 to 2012 (see, for example, Supplementary Fig. 1).

Some species' occurrence records were sparse, particularly after 1980, so we used simulations to test the sensitivity of estimated range-warming trends to sampling gaps (Supplementary Table 4). We first generated samples that were randomly distributed at HC grid points and evenly distributed among the years 1958–2012 (the full dataset). The total sample size was $N = 220, 550, 1,100$ or $2,200$, a range spanning most species' sample sizes (Supplementary Table 1). For each N, we randomly generated 1,000 full datasets and 1,000 partial datasets omitting data from each of 18 different 10- or 20-year segments. For each dataset, we estimated the temperature trend using linear regressions of $T'_{b_{HC}}$ versus year from 1958

to 2012. Finally, for each N we did a one-way analysis of variance with multiple comparisons to test whether the mean temperature trends in the partial datasets differed from the mean trend in the full datasets. The estimated temperature trends were sensitive to data gaps in the 1960s, 1970s and 2000s but insensitive to data gaps in the 1980s and 1990s (Supplementary Table 4), both decades when the NWA spatial mean temperatures closely matched the long-term trend (Extended Data Fig. 2). Gaps in the species occurrence data generally coincided with the period when simulated data gaps were benign, suggesting that the estimated range warming trends were unbiased.

Climate velocity. Previous studies found that some species' ranges track the local climate velocity[4], so our analyses included velocities of T_b. We computed climate velocities as:

$$\frac{\partial \text{Latitude}}{\partial t} = \frac{\frac{\partial \overline{T'_{b_{HC}}}}{\partial t}}{\frac{\partial \overline{T'_{b_{HC}}}}{\partial \text{Latitude}}} \quad (4)$$

$$\frac{\partial \text{Longitude}}{\partial t} = \frac{\frac{\partial \overline{T'_{b_{HC}}}}{\partial t}}{\frac{\partial \overline{T'_{b_{HC}}}}{\partial \text{Longitude}}} \quad (5)$$

where the overbars indicate time averaging. Temporal gradients were calculated as the linear regression slope of $T'_{b_{HC}}$ versus year at each grid point. Spatial gradients were computed on long-term $\overline{T'_{b_{HC}}}$ using each vertex and at least five adjacent points on the terrain-following grid using Delaunay triangulation[48]. The velocities of T_b varied with bathymetry, and in the MAB, they diverged at mid-shelf associated with the cold pool (Extended Data Fig. 4). For each species, we interpolated ∂latitude$/\partial t$ and ∂longitude$/\partial t$ to the occurrence locations and averaged them to estimate the mean climate velocities across each species' range (Fig. 3g,h and Extended Data Fig. 1d,e).

Spawning phenology. Adults' spawning phenology depends on how T_b varies seasonally. We represented seasonal cycles of T_b using daily mean temperatures from the HC. At each grid point, we smoothed the daily temperature outputs with a 28-day, central moving average to get spatially resolved seasonal cycles, $T_{b_{HCseason}}(x, y, t_d, t)$, where t_d is day of the year. Daily temperatures contain the same systematic model bias as annual temperatures, so we bias- and trend-corrected them as described above:

$$T'_{b_{HCseason}}(x, y, t_d, t) = T_{b_{HCseason}}(x, y, t_d, t) - \tau_{HC}(t) + \tau_{WOD}(t). \quad (6)$$

We used $T'_{b_{HCseason}}$ to calculate the first day of spawning at potential temperature thresholds for all grid points and years. The spawning temperature threshold is unknown in most species (see Supplementary Table 2 for the exceptions), so we used four likely thresholds with onset dates at t_8, t_{10}, t_{12} and t_{14}, where the subscripts indicate the threshold temperature (°C). To quantify the potential changes in species' spawning phenology, we interpolated the onset dates for each temperature threshold to occurrence locations and then estimated trends using linear regressions of the onset dates at the occurrence locations versus year (Fig. 3i–l and Extended Data Fig. 1g–j).

Despite the limitations of the WOD temperature observations, the overall patterns in estimated range warming and phenological shifts (Fig. 3 and Extended Data Fig. 1) were insensitive to details of HC bias correction. The ROMS model accurately captured the regional spatial variation of temperature that dominated temperature changes across shifting ranges. As a result, our analysis identified qualitatively similar patterns using the temperature data itself, the uncorrected model, the model with an alternative bias correction and the model with the spatially averaged bias correction used here (equations (3)–(6)). Only the latter is presented due to space limitations, but the patterns are robust because species' range warming was dominated by ranges shifting to warmer locations.

Statistics. We tested whether the aggregated benthic species' range shift velocities were correlated with climate velocities or phenological shift rates using single linear regressions. The dependent variables included the range shift velocities in latitude/longitude coordinates for the NWA and MAB and in shelf coordinates for the MAB (Fig. 3a–d and Extended Data Fig. 1a,b). The independent variables included the latitudinal or longitudinal climate velocities averaged over the occurrence locations in the NWA or MAB for each species (Fig. 3g,h and Extended Data Fig. 1d,e) or the estimated phenological shift rates for the four spawning temperatures (Fig. 3i–l and Extended Data Fig. 1g–j). The regressions indicated that species' range shift velocities were uncorrelated with climate velocity except along longitude in the MAB ($P = 0.02$, $R^2 = 0.15$; Extended Data Fig. 5). In that region, ∂longitude$/\partial t$ diverges at mid-shelf, and the correlation would have occurred coincidentally as species' ranges contracted from the outer shelf (where ∂Lon$/\partial t$ is positive) to the inner shelf (where ∂longitude$/\partial t$ is negative) (Extended Data Fig. 4e). In contrast, range shift velocities were often correlated with phenological shift rates, and 11 out of 16 regressions showed a positive correlation (Extended Data Fig. 7).

Transport mechanisms in the MAB. Spawning phenology affects larval transport via seasonal variation in wind-driven ocean currents, so we quantified the climatology of winds. Wind data for 1958–2007 were taken from the interannually varying Coordinated Ocean Research Experiments version 2 reanalysis[49]. The wind reanalysis was coarsely resolved but varied more seasonally than spatially in the MAB, so we used wind from a single, central grid point (39.047° N, 73.125° W). The wind velocities were rotated 28 degrees east of north to align with the average coastline orientation and then low-pass filtered using a Lanczos filter with a cut-off period of 30 days and a half-window width of 45 days. We used the filtered data to compute mean ± 1 s.d. climatology (Fig. 2a). Although there have been no long-term trends in winds or waves in our study region[38], we checked for long-term trends in wind seasonal cycles. We did linear regressions of monthly average wind speeds over the 50-year record and found no significant trends in either component of the wind velocity. We also found no trend in the seasonal variability of the wind. We therefore used mean climatology (Fig. 2a) to evaluate seasonal variation in along-shelf winds encountered by larvae.

Spawning phenology also affects larval transport via seasonal variation in buoyancy-driven flow, so we quantified the climatology of freshwater river discharge. River data for 1950 to 2017 were obtained from US Geological Survey Water Data for the Nation[50] and combined for the Northeast Basin, including the Connecticut (CT), Raritan (NJ), Passaic (NJ), Mohawk (NY), Hudson at Fort Edward (NY), Delaware (NJ) and the four largest rivers discharging through Chesapeake Bay: Potomac (DC), James (VA), Rappahannock (VA) and Susquehanna (MD). We summed the mean daily discharge from all rivers and used daily totals to compute monthly mean ± 1 s.d. outflows. We also checked for long-term trends using linear regressions of monthly average outflow over the 67-year record and found no significant trends except for a modest increase in July, when river discharge is at a minimum. We therefore used the mean climatology (Fig. 2b) to represent the seasonal variation in river discharge encountered by larvae.

Winds and river discharge are forcing mechanisms, but larvae are transported by the resulting currents, so we also estimated the climatology of along-shelf flow. Along-shelf currents are seasonal even when depth averaged[28], whereas across-shelf flow is weaker and depends more on vertical position in the water column, so we focused on transport by the stronger along-shelf currents. We estimated the seasonality of along-shelf flow using data presented in refs. [28,51] from ten moorings located shorewards of the 60 m isobath. For each mooring, the annual mean was taken from Table 1 in ref. [51] and added to the seasonal signal on the basis of current ellipses from Table 1 in ref. [28]. We combined data from the ten moorings to estimate the daily mean ± 1 s.d. of along-shelf velocity in the MAB (Fig. 2c). Note that these estimates of along-shelf flow are based on harmonic analysis and probably underestimate the seasonal variation associated with peak downwelling winds and river discharge.

We used the harmonic analysis of along-shelf currents in the MAB to quantify how phenological shifts in spawning have changed larval advection. For each species, we first estimated the dates of spawning onset at different temperature thresholds (t_8, t_{10}, t_{12} and t_{14}) in each year from 1960 to 2010 using regression parameters (see 'Spawning phenology'). We assumed that most larvae are released at the onset of spawning and are transported for a fixed larval duration; pelagic larval durations (PLDs) vary but are typically about one month[52]. We averaged the along-shelf velocities over PLDs of 30 days following each date of spawning onset (Extended Data Fig. 8) and then estimated the trend in larval transport from linear regression of the mean transport velocity versus year. Finally, we did linear regressions of the estimated trends in transport velocity versus the observed adult range shifts. The regressions were significant using all estimates associated with shifts to earlier spawning and using estimates associated with seven species' known spawning temperatures (Fig. 4b and Supplementary Table 2). We tested for sensitivity to PLD by repeating this analysis using PLDs of 2 to 90 days. The regressions for earlier spawning estimates were significant for all PLDs longer than two weeks, and the regressions for known spawning temperatures were significant for PLDs up to 50 days.

Range area change. Marine species generally fill the range of thermally tolerable latitudes[3], yet a range can expand in latitude while becoming compressed in longitude or depth. In the NWA, we recorded changes in total range extent from 1951–1980 to 1981–2010 for species with ≥100 occurrence observations in each 30-year period. For each period, we calculated the total range extents as the minimum to maximum latitude, longitude, depth and $T'_{b_{HC}}$ at the occurrence locations, excluding the outer 2% of each metric's distribution to eliminate outliers (Extended Data Fig. 9). In the MAB, the relatively simple coastline enabled us to quantify changes in species' occupied area from 1951–1980 to 1981–2010. This analysis included only 26 species with ≥200 occurrence observations in the MAB in each period (Supplementary Table 1). For each species and period, we estimated the occupied area enclosed by a polygon drawn around the occurrence locations using MATLAB's (R2018a) boundary function. The polygons were drawn with maximum shrinkage to limit the included land area between nearshore occurrence locations. For each species and year, we also estimated thermally tolerable areas as the number of HC grid points in each region where the annual

average temperatures were within the species' tolerable ranges. Tolerable ranges were defined here as the minimum to maximum $T'_{b_{HC}}$ at the occurrence locations (Supplementary Table 5). Finally, we calculated the percentage change in occupied area and tolerable area from the first to the second 30-year period (Extended Data Fig. 10).

Reporting Summary. Further information on research design is available in the Nature Research Reporting Summary linked to this article.

Data availability
All data analysed in this paper are publicly available. The species occurrence data are available from OBIS (https://www.iobis.org). The bathymetry data are available from NOAA (https://doi.org/10.7289/V5C8276M). The river data are available from USGS (http://waterdata.usgs.gov/nwis/). The wind data are available from NCAR (https://climatedataguide.ucar.edu/climate-data/core v2-air-sea-surface-fluxes). The temperature data are available from WOD (https://www.nodc.noaa.gov/OC5/WOD/pr_wod.html) and from Rutgers (https://esm.rutgers.edu/). All data used in the analyses are available in condensed form on Zenodo (https://doi.org/10.5281/zenodo.3934122).

Code availability
All codes necessary for data analysis and figure generation are available on Zenodo (https://doi.org/10.5281/zenodo.3946797).

References
39. *Ocean Biogeographic Information System* (Intergovernmental Oceanographic Commission of UNESCO, 2018); www.iobis.org
40. Tingley, M. W. & Beissinger, S. R. Detecting range shifts from historical species occurrences: new perspectives on old data. *Trends Ecol. Evol.* **24**, 625–633 (2009).
41. Wigley, R. L. & Theroux, R. B. *Atlantic Continental Shelf and Slope of the United States; Macrobenthic Invertebrate Fauna of the Middle Atlantic Bight Region; Faunal Composition and Quantitative Distribution* Professional Paper No. 529-N (USGS, 1981).
42. Amante, C. & Eakins, B. W. *ETOPO1 1 Arc-Minute Global Relief Model: Procedures, Data Sources and Analysis* Technical Memorandum NESDIS NGDC-24 (National Geophysical Data Center, NOAA, 2009); https://doi.org/10.7289/V5C8276M
43. Loarie, S. R. et al. The velocity of climate change. *Nature* **462**, 1052–1057 (2009).
44. Kang, D. & Curchitser, E. N. Gulf stream eddy characteristics in a high-resolution ocean model. *J. Geophys. Res. Oceans* **118**, 4474–4487 (2013).
45. Narváez, D. A. et al. Long-term dynamics in Atlantic surfclam (*Spisula solidissima*) populations: the role of bottom water temperature. *J. Mar. Sys.* **141**, 136–148 (2015).
46. Chen, Z., Curchitser, E., Chant, R. & Kang, D. Seasonal variability of the cold pool over the Mid-Atlantic Bight continental shelf. *J. Geophys. Res. Oceans* **123**, 8203–8226 (2018).
47. D'Errico, J. inpaint_nans (MATLAB Central File Exchange, 2019); https://www.mathworks.com/matlabcentral/fileexchange/4551-inpaint_nans
48. Gypaets trigradient2 (GitHub, 2020); https://www.github.com/Gypaets/trigradient2
49. Yeager, S. & NCAR Staff *The Climate Data Guide: COREv2 Air-Sea Surface Fluxes* (UCAR, 2016); https://climatedataguide.ucar.edu/climate-data/core v2-air-sea-surface-fluxes
50. *National Water Information System Data* (USGS, 2016); http://waterdata.usgs.gov/nwis/
51. Lentz, S. J. Observations and a model of the mean circulation over the Middle Atlantic Bight continental shelf. *J. Phys. Oceanogr.* **38**, 1203–1221 (2008).
52. Shanks, A. L. Pelagic larval duration and dispersal distance revisited. *Biol. Bull.* **216**, 373–385 (2009).

Author contributions
H.L.F., R.J.C. and G.P.G. designed the study. H.L.F., R.J.C., E.J.H. and E.Y.C. compiled and analysed the data. E.N.C. contributed data. H.L.F. and R.J.C. wrote the paper.

Competing interests
The authors declare no competing interests.

Additional information
Extended data is available for this paper at https://doi.org/10.1038/s41558-020-0894-x.

Supplementary information is available for this paper at https://doi.org/10.1038/s41558-020-0894-x.

**Correspondence and requests for materials** should be addressed to H.L.F.

Peer review information *Nature Climate Change* thanks Matthew Ferner and Jorge García Molinos for their contribution to the peer review of this work.

**Reprints and permissions information** is available at www.nature.com/reprints.
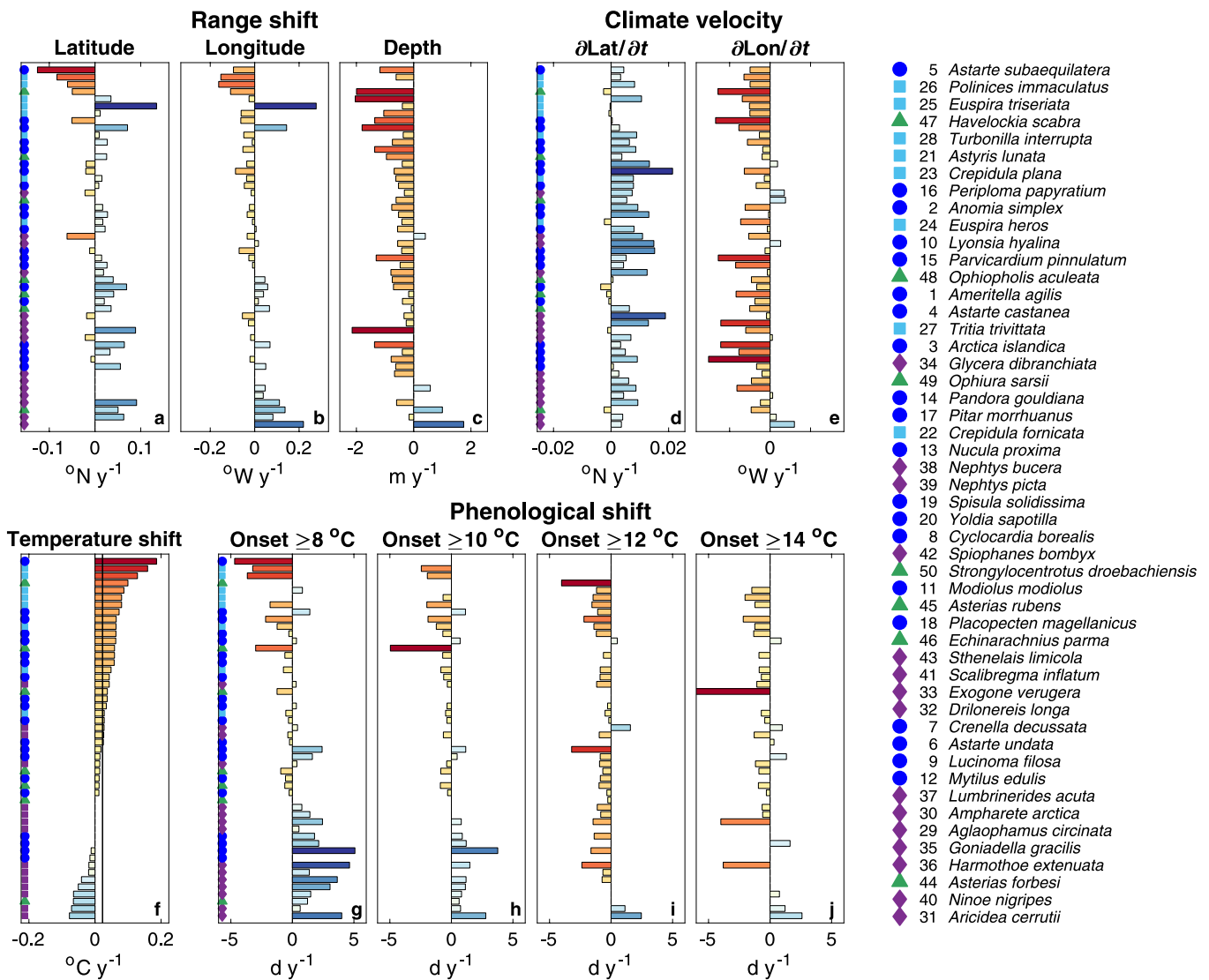
Extended Data Fig. 1 | In NWA region, most ranges shifted westward and into shallower, warmer regions with earlier spawning onset. Bars show trends in latitude (**a**), longitude (**b**), and depth (**c**) computed from observed occurrence locations versus year (1950–2015) for each species. Mean climate velocities (**d**,**e**) and trends in bottom water temperature (**f**) and onset dates for spawning temperatures 8 to 14 °C (**g-j**) computed from model hindcast at occurrence locations versus year (1958–2012). Vertical line (**f**) indicates mean warming trend in temperature record. Trends included only if significant at $\alpha = 0.05$. Symbols indicate taxon (blue circles, bivalves; cyan squares, gastropods; purple diamonds, polychaetes; green triangles, echinoderms); legend indicates species. Lon, longitude; Lat, latitude.
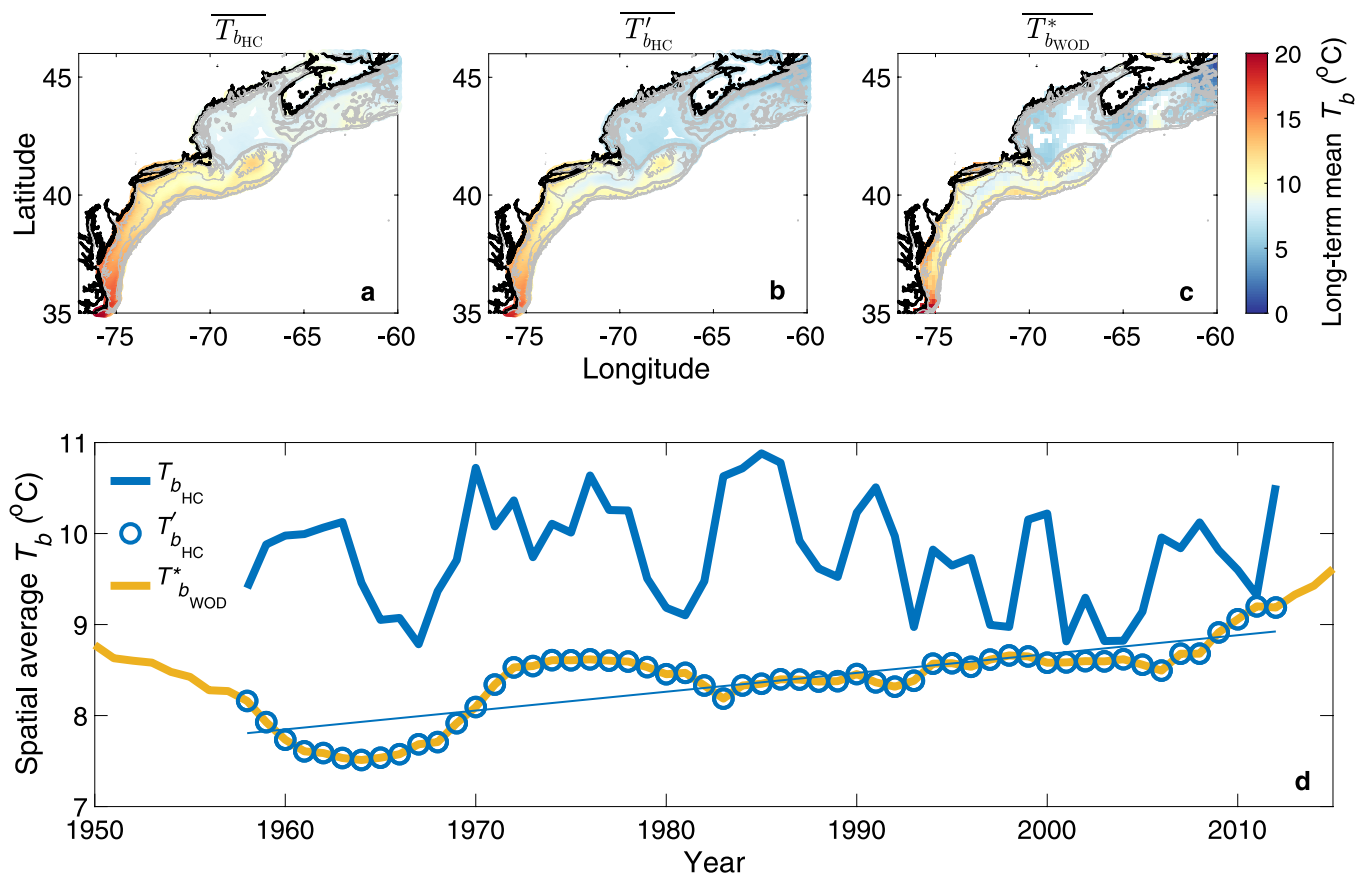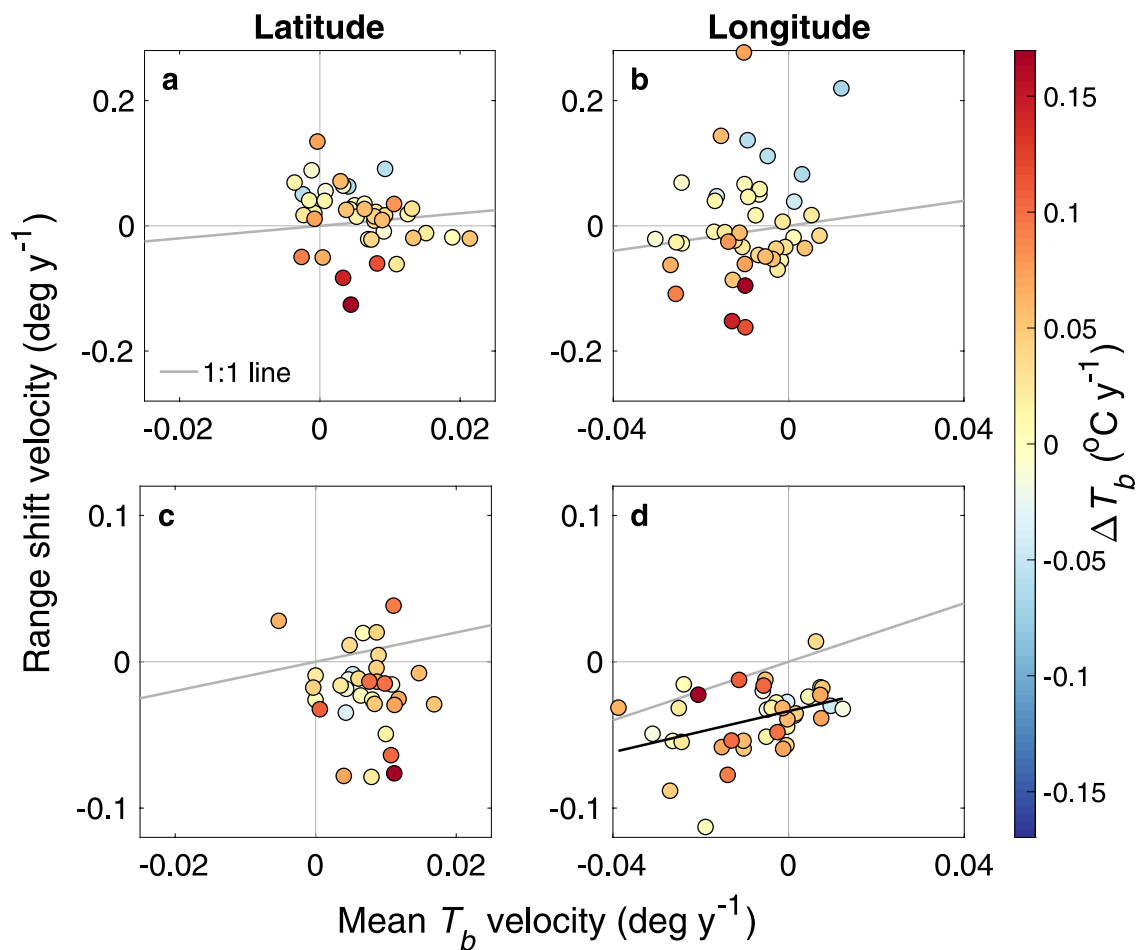
Extended Data Fig. 2 | Bottom water temperatures from corrected model (HC) have mean spatial pattern and long-term trend matching observations (WOD). Maps show long-term mean bottom water temperatures from uncorrected HC (**a**, $T_{b_{HC}}$), bias- and trend-corrected HC (**b**, $T'_{b_{HC}}$), and re-weighted WOD data (**c**, $T^*_{b_{WOD}}$). **d**) Time series of spatial mean annual bottom water temperature from uncorrected HC (thick blue line), corrected HC (blue circles), and WOD (yellow line). Bias correction replaces the spatial mean annual temperature of HC with that of WOD data (Eq. (3)), preserving the spatial variability in warming. Thin blue line is linear regression of corrected HC or WOD (1958–2012) temperatures versus year (slope = 0.021ºC y⁻¹; $p < 10^{-12}$; R^2 = 0.65). Uncorrected HC temperature has no significant trend versus year.
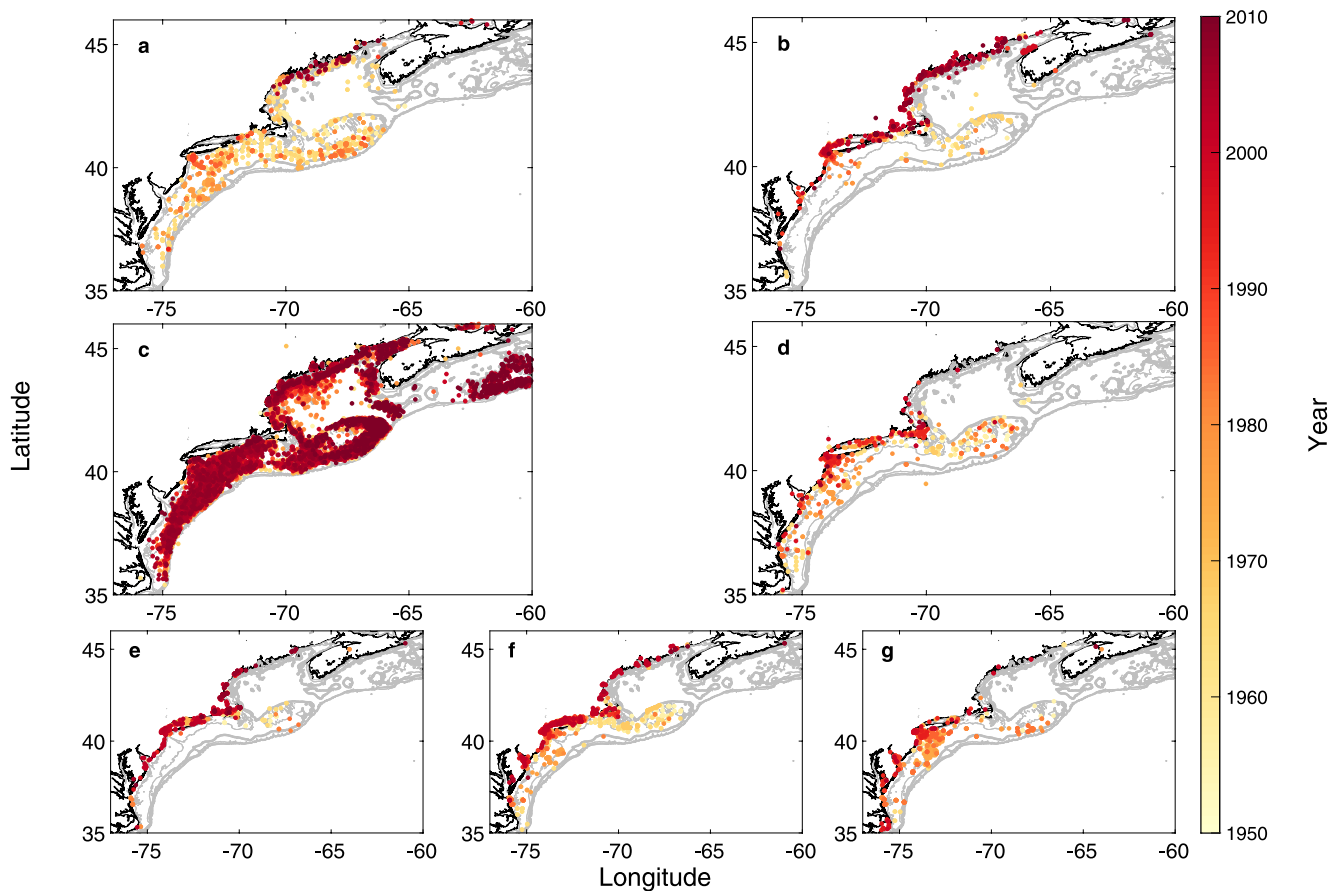
Extended Data Fig. 3 | Occurrence distributions over time are shown for selected species with known spawning temperatures (Supplementary Table 2).
Includes four commercial (fished) bivalves (**a**, 03 *Arctica islandica*; **b**, 12 *Mytilus edulis*; **c**, 18 *Placopecten Magellanicus*; **d**, 19 *Spisula solidissima*), two snails (**e**, 22 *Crepidula fornicata*; **f**, 27 *Tritia trivittata*), and a polychaete (**g**, 34 *Glycera dibranchiata*) where numbers indicate ordering in Supplementary Table 1. Dots are recorded occurrences, and colors indicate the year. Some dots overlap; see Supplementary Table 1 for total number of records.
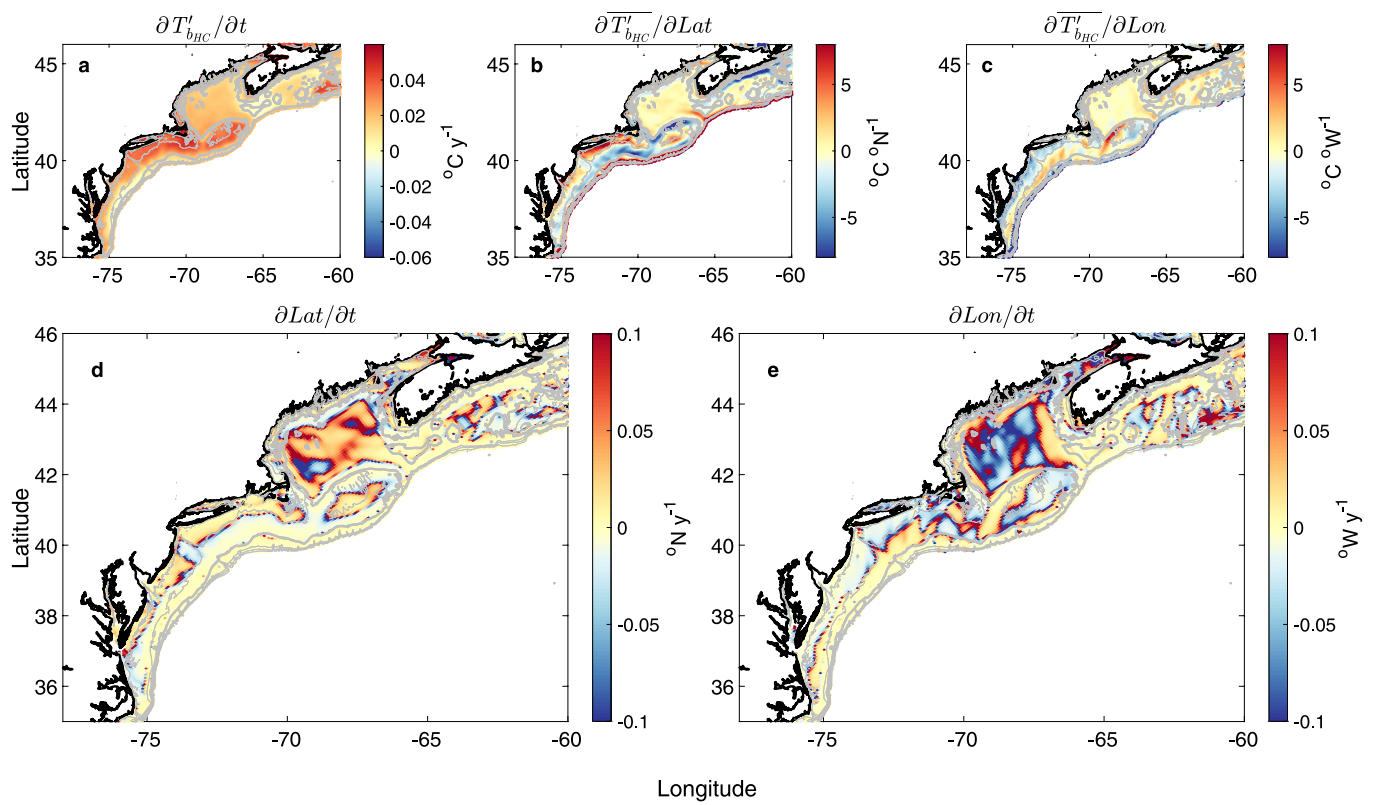
Extended Data Fig. 4 | Climate velocities of bottom water temperature varied with bathymetry and diverged mid-shelf in MAB. Maps show $\partial T'_{b_{HC}}/\partial t$ (**a**), $\partial \overline{T'_{b_{HC}}}/\partial \mathrm{Lat}$ (**b**), $\partial \overline{T'_{b_{HC}}}/\partial \mathrm{Lon}$ (**c**), $\partial \mathrm{Lat}/\partial t$ (**d**), and $\partial \mathrm{Lon}/\partial t$ (**e**) computed from corrected hindcast annual mean temperatures (Eqns. (4)-(5)). Lon, longitude; Lat, latitude.

Extended Data Fig. 5 | Range shift velocities were mostly uncorrelated with mean bottom water temperature velocities (climate velocities) across species ranges in NWA and MAB regions. Data from NWA (**a,b**) and MAB (**c,d**). Range shift velocities are from Fig. 3a,b or Extended Data Fig. 1a,b, and mean climate velocities (Eq. (4)–(5)) are from Fig. 3g,h or Extended Data Fig. 1d,e. Positive velocities are northward for latitude and eastward for longitude. Symbols are estimates for each species where trends in latitude (**a,c**) or longitude (**b,d**) are significant; **c,d** omit species sparse in MAB (Supplementary Table 1). Colors indicate associated trends in $T'_{b_{HC}}$ at occurrence locations. Diagonal grey lines are 1:1; black line (**d**) is regression significant at $\alpha = 0.05$ ($p = 0.02$, $R^2 = 0.15$).
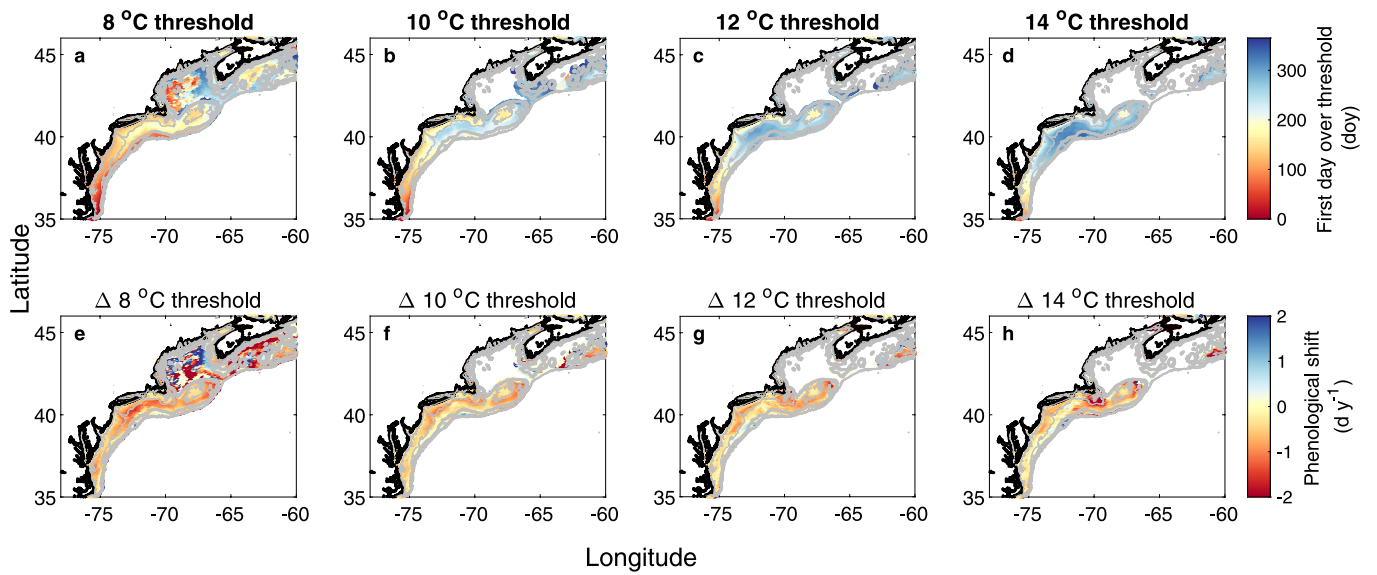
Extended Data Fig. 6 | Spawning would occur earliest in the southern part of the study area but probably has shifted earlier due to warming throughout the region. Maps show long-term averages (**a**-**d**) and temporal trends (**e**-**h**) in onset dates for spawning at four temperature thresholds (t_8, t_{10}, t_{12}, t_{14}) in the Northwest Atlantic region. Onset dates were calculated from corrected HC climatology, and trends were calculated from linear regression of onset dates versus year at each grid point. Regions with no color are always below the indicated temperature threshold.
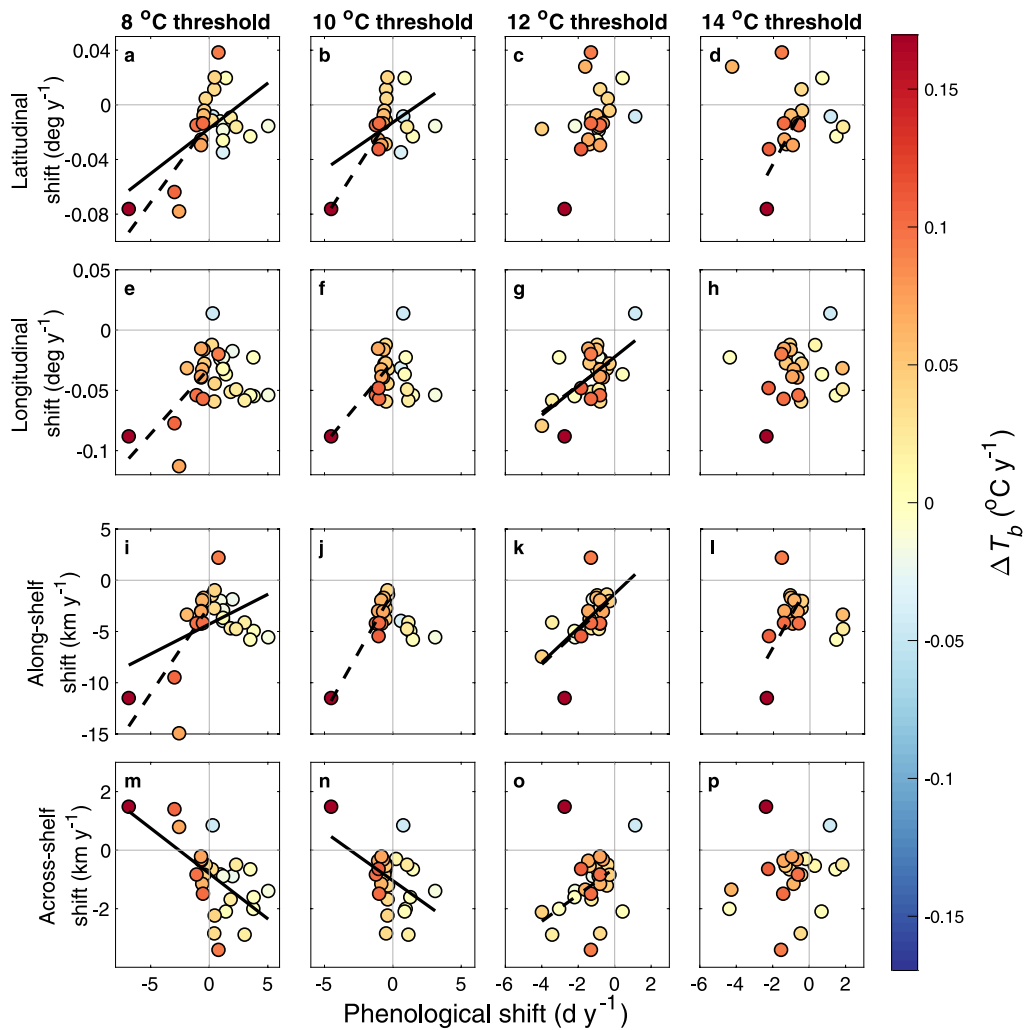
Extended Data Fig. 7 | Range shift velocities were mostly positively correlated with phenological shift rates in the Middle Atlantic Bight. Range shift velocities shown in Lat/Lon (**a-h**) and shelf coordinates (**i-p**) versus phenological shift rates for four potential spawning temperatures (8, 10, 12, and 14 °C). Range shift velocities are from Fig. 3a-d, and phenological shift rates are from Fig. 3i-l. Symbols are estimates for each species where significant, omitting species sparse in MAB (Supplementary Table 1). Colors indicate associated trends in T_b at locations of occurrence. Black lines are linear regressions of all data (solid) or lower left quadrant only (dashed) where significant at $\alpha = 0.05$.
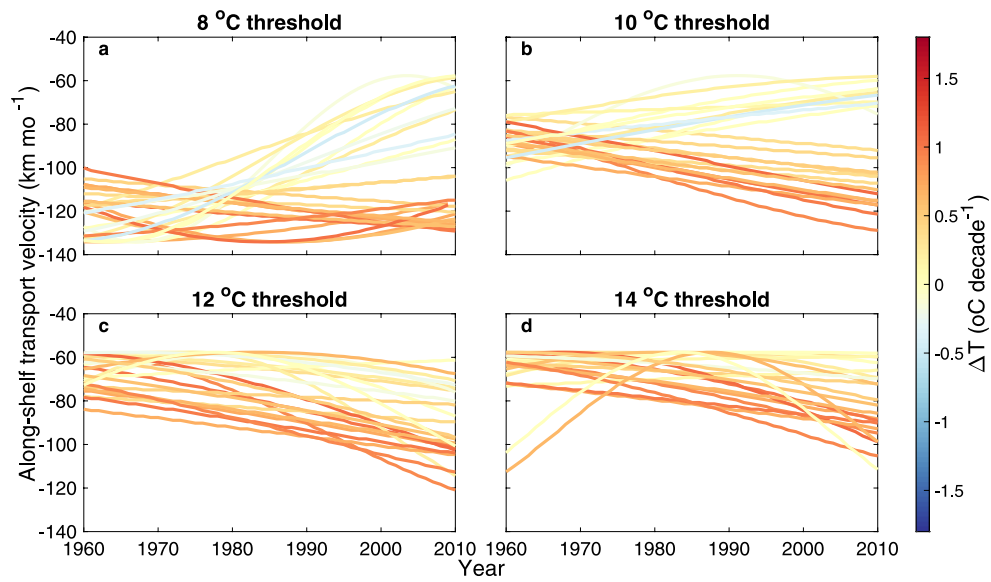
Extended Data Fig. 8 | Most estimated phenological shifts from 1960 to 2010 would result in increasingly negative (down-shelf) mean larval transport velocities. Mean along-shelf transport velocity versus year from 1960 to 2010, averaged over the 30 days following estimated spawning onset dates. Negative velocities indicate down-shelf transport. Lines are estimates for individual species spawning at four potential temperature thresholds (**a-d**). Includes estimates where both phenological shift and range shift were significant at $\alpha < 0.05$. Omits species sparse in MAB or sparse or absent in MAB after 1990 (Supplementary Table 1). Line colors indicate rate of range warming in MAB from observations in Fig. 3f.
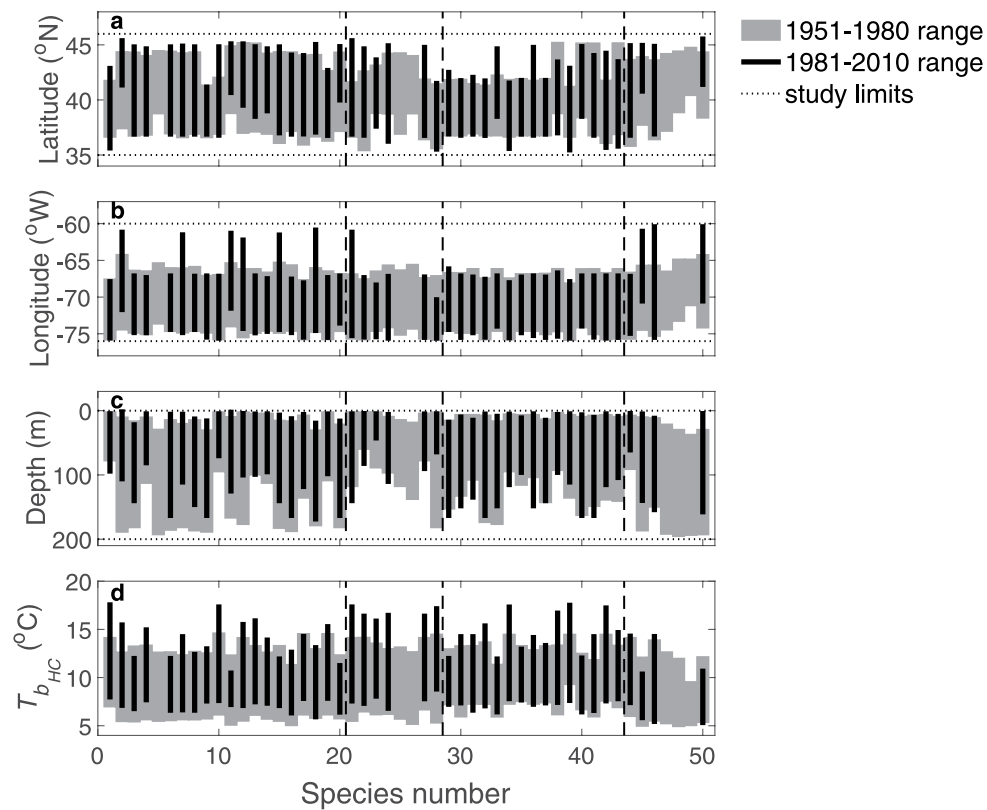
Extended Data Fig. 9 | Most species' total range extents changed over time within NWA. Range extents (vertical bars) of Lat (**a**), Lon (**b**), depth (**c**), and $T'_{b_{HC}}$ (**d**) are plotted versus species number: #1–20, bivalves; #21–28, gastropods; #29–43, polychaetes; #1–50, echinoderms (Supplementary Table 1). Bars show 98% of data for 1951-1980 (grey) and 1981-2010 (black). The outer 2% of distributions were removed to eliminate outliers. Includes species with > 100 occurrence observations in each time period; absent bars indicate species with too few data in later time period. Range extents were estimated from occurrence locations; ranges of annual average bottom water temperatures were estimated from $T'_{b_{HC}}$.
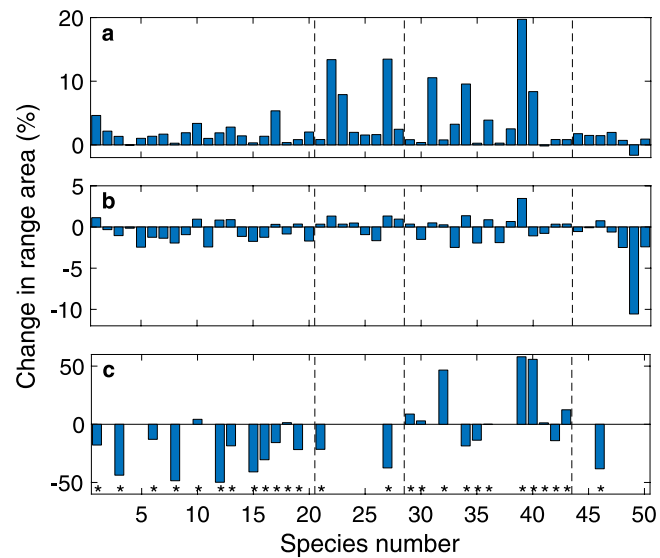
Extended Data Fig. 10 | Species' ranges have contracted even where tolerable range area has expanded. a-b) Change in tolerable habitat area from 1951-1980 to 1981-2010 within NWA (**a**) or MAB (**b**), estimated from corrected HC assuming all previously occupied range temperatures (Supplementary Table 5) are tolerable. **c)** Change in occupied range area from 1951-1980 to 1981-2010, estimated from occurrence locations within MAB, for species with > 200 occurrence observations in each time period as indicated by asterisks above x-axis (species number). Species' occupied areas changed by an average of − 24.5% for bivalves (#1–20), − 29.5% for gastropods (#21–28), 12.7% for polychaetes (#29–43), and − 38.2% for one echinoderm with sufficient data. For species with estimates in **c**, tolerable ranges increased overall by an average of 3.3% in NWA and 0.02% in MAB. Within MAB, changes in occupied range area and tolerable range area were uncorrelated.

naturereseearch

Corresponding author(s):   Heidi L. Fuchs

Last updated by author(s): 07/16/2020

Reporting Summary

Nature Research wishes to improve the reproducibility of the work that we publish. This form provides structure for consistency and transparency in reporting. For further information on Nature Research policies, see Authors & Referees and the Editorial Policy Checklist.

Statistics

For all statistical analyses, confirm that the following items are present in the figure legend, table legend, main text, or Methods section.

n/a	Confirmed	
☐	☒	The exact sample size (*n*) for each experimental group/condition, given as a discrete number and unit of measurement
☐	☒	A statement on whether measurements were taken from distinct samples or whether the same sample was measured repeatedly
☐	☒	The statistical test(s) used AND whether they are one- or two-sided *Only common tests should be described solely by name; describe more complex techniques in the Methods section.*
☐	☒	A description of all covariates tested
☐	☒	A description of any assumptions or corrections, such as tests of normality and adjustment for multiple comparisons
☐	☒	A full description of the statistical parameters including central tendency (e.g. means) or other basic estimates (e.g. regression coefficient) AND variation (e.g. standard deviation) or associated estimates of uncertainty (e.g. confidence intervals)
☒	☐	For null hypothesis testing, the test statistic (e.g. *F*, *t*, *r*) with confidence intervals, effect sizes, degrees of freedom and *P* value noted *Give P values as exact values whenever suitable.*
☒	☐	For Bayesian analysis, information on the choice of priors and Markov chain Monte Carlo settings
☒	☐	For hierarchical and complex designs, identification of the appropriate level for tests and full reporting of outcomes
☒	☐	Estimates of effect sizes (e.g. Cohen's *d*, Pearson's *r*), indicating how they were calculated

Our web collection on statistics for biologists contains articles on many of the points above.

Software and code

Policy information about availability of computer code

Data collection	No original data were collected.
Data analysis	All data were analyzed using Matlab (MathWorks) software. All code are provided on Zenodo (doi: 10.5281/zenodo.3946797).

For manuscripts utilizing custom algorithms or software that are central to the research but not yet described in published literature, software must be made available to editors/reviewers. We strongly encourage code deposition in a community repository (e.g. GitHub). See the Nature Research guidelines for submitting code & software for further information.

Data

Policy information about availability of data

All manuscripts must include a data availability statement. This statement should provide the following information, where applicable:

- Accession codes, unique identifiers, or web links for publicly available datasets
- A list of figures that have associated raw data
- A description of any restrictions on data availability

All data used in the manuscript are publicly available on the World Wide Web. Species occurrence data are available from OBIS (https://www.iobis.org). Bathymetry data are available from NOAA (doi:10.7289/V5C8276M). River data are available from USGS (http://waterdata.usgs.gov/nwis/). Wind data are available from NCAR (https://climatedataguide.ucar.edu/climate-data/corev2-air-sea-surface-fluxes). Temperature data are available from WOD (https://www.nodc.noaa.gov/OC5/WOD/pr_wod.html) and from Rutgers (https://esm.rutgers.edu/). All data are provided in condensed form on Zenodo (doi: 10.5281/zenodo.3934122).

Field-specific reporting

Please select the one below that is the best fit for your research. If you are not sure, read the appropriate sections before making your selection.

☐ Life sciences   ☐ Behavioural & social sciences   ☒ Ecological, evolutionary & environmental sciences

For a reference copy of the document with all sections, see nature.com/documents/nr-reporting-summary-flat.pdf

Ecological, evolutionary & environmental sciences study design

All studies must disclose on these points even when the disclosure is negative.

Study description	This study used publicly available data to analyze trends in benthic species' occurrence locations and associated bottom water temperatures from 1950 to 2015. For each species analyzed, we estimated local climate velocities and the timing of larval release (phenology) over a range of likely spawning temperatures. Shifts in spawning phenology were related to seasonal variation in physical transport driven by winds and river discharge. Estimated phenology-driven increases in larval along-shelf transport were positively correlated with observed adults' along-shelf range shifts.
Research sample	We analyzed observed occurrences of adults or juveniles of 50 benthic invertebrates (bivalves, gastropods, polychaete worms, and echinoderms) that are relatively abundant on the Northwest Atlantic continental shelf. All occurrence data available from OBIS were included. The total number of occurrence records and date range for each species is listed in Supplementary Table 1.
Sampling strategy	No original samples were collected.
Data collection	No original data were used. Species occurrence data were downloaded by H.L. Fuchs. Bathymetry, temperature, wind, and river data were downloaded by E.J. Hunter.
Timing and spatial scale	Data were collected from 1950 to 2015 from the continental shelf at depths <200 m in the Northwest Atlantic between 35° and 46° N and -60° and -76° W and in a subset of this region -- the Middle Atlantic Bight -- between 35° and 41.6° N and -76° and-70° W.
Data exclusions	Observed bottom water temperatures (from WOD) were excluded if the reported measurement depth was greater than the local water depth or if bottom water temperature was < 0 °C or > 30 °C, either of which indicates a faulty measurement. Species with fewer than 100 records in the MAB were omitted from MAB analyses. Six species were excluded from the analysis shown in Fig. 4 because they were sparse or absent within Middle Atlantic Bight (MAB) after 1990. Species with fewer than 200 records in either of two time periods (1951-1980 and 1981-2010) were excluded from estimates of MAB range area change.
Reproducibility	All observations were previously collected by other researchers over a 65-year period. Environmental conditions and species' locations vary in time and have been altered by ocean warming, therefore it would impossible to reproduce identical measurements. However, the analyses were all done via computer code and are 100% reproducible.
Randomization	N/A -- Each species was analyzed individually, and all observations were used.
Blinding	N/A -- No grouping was done, and all observations were used.

Did the study involve field work?   ☐ Yes   ☒ No

Reporting for specific materials, systems and methods

We require information from authors about some types of materials, experimental systems and methods used in many studies. Here, indicate whether each material, system or method listed is relevant to your study. If you are not sure if a list item applies to your research, read the appropriate section before selecting a response.

Materials & experimental systems

n/a	Involved in the study
☒ ☐	Antibodies
☒ ☐	Eukaryotic cell lines
☒ ☐	Palaeontology
☒ ☐	Animals and other organisms
☒ ☐	Human research participants
☒ ☐	Clinical data

Methods

n/a	Involved in the study
☒ ☐	ChIP-seq
☒ ☐	Flow cytometry
☒ ☐	MRI-based neuroimaging